Modeling of Two Sub-reach Water Systems: Application to Navigation Canals in the North of France

Pau Segovia[1,2], Klaudia Horváth[3], Lala Rajaoarisoa[1], Fatiha Nejjari[2], Vicenç Puig[2] and Eric Duviella[1]
[1]*Unité de Recherche en Informatique et Automatique, IMT Lille Douai, Lille, France*
[2]*Automatic Control Department, Universitat Politècnica de Catalunya, Terrassa, Spain*
[3]*Department of Mechanical Engineering, Eindhoven University of Technology, Eindhoven, The Netherlands*

Keywords: Large-scale Systems, Water Systems, Saint-Venant Equations, Modeling, IDZ Models.

Abstract: Inland navigation networks are large-scale systems that can be described by using the nonlinear Saint-Venant partial differential equations. However, as there is no analytical solution for them, simplified models are used instead for modeling purposes. This work addresses the modeling of two sub-reach systems by means of the well-known Integrator Delay Zero model. Two main scenarios are considered: in the first one, the two partial models are independently computed one from each other; the second one uses previous knowledge of the whole two sub-reach system in order to ensure the flow consistency along the system. The application of these two methodologies to a part of the navigation network in the north of France serves as the case study for this work.

1 INTRODUCTION

Inland navigation networks cover more than 38000 km in Europe and are used principally for transport. The navigation transport takes part in the Trans-European network program (TEN-T[1]), which promotes *the development of transport infrastructure policies to close the gaps between Member States' transport networks and to guarantee seamless transport chains for passengers and freight*. In France, an intensification in the use of inland waterways is expected in the near future. The gauge of the allowed boats and the navigation schedule will be risen up. Hence, constraints on the inland waterway management will be more severe.

The accommodation of navigation requires the control of the water levels in each part of the navigation network, which is composed of several interconnected reaches that represent portions of a water stream between at least two hydraulic structures such as locks. These reaches are large-scale, free-surface systems that exhibit large delays between the generation of an upstream input and its measurement along the water course and at the downstream end of the reach. Some perturbations can travel back and forth, resulting in resonance phenomena. The dynamics of the reach can be accurately described by the Saint-Venant's partial differential equations (Chow, 1959). However, as there is no known analytical solution for these equations, simplified models such as transfer functions (Litrico and Georges, 1999) or the Integrator Delay (ID) model (Schuurmans et al., 1999) are used instead. These models are designed by considering some assumptions on the linearity of the reach dynamics. The ID model was improved by considering an additional zero that allows taking into account high frequency phenomena. The obtained Integrator Delay Zero model (IDZ) was tested and compared with the ID model on several canals (Litrico and Fromion, 2004). More recently, an Integrator Resonance model (IR) has been proposed (van Overloop et al., 2010), (Horváth et al., 2014b) and (van Overloop et al., 2014) to reproduce the resonance phenomena. Gray-box models can be used when lacking prior knowledge of the physical characteristics of canals, such as dimensions or the Manning-Strickler coefficient (Duviella et al., 2013) and (Horváth et al., 2014a). Finally, approaches based on linear parameter-varying models or multi-models that enable to take into account the nonlinearities due to the consideration of large operating ranges were proposed (Duviella et al., 2007), (Duviella et al., 2010), (Bolea et al., 2014) and (Bolea and Puig, 2016).

[1]http://ec.europa.eu/transport/themes/infrastructure/ten-t-guidelines/index_en.htm

Segovia, P., Horváth, K., Rajaoarisoa, L., Nejjari, F., Puig, V. and Duviella, E.
Modeling of Two Sub-reach Water Systems: Application to Navigation Canals in the North of France.
DOI: 10.5220/0006418604590467
In *Proceedings of the 14th International Conference on Informatics in Control, Automation and Robotics (ICINCO 2017) - Volume 1*, pages 459-467
ISBN: 978-989-758-263-9

Many man-made, hydraulic structures such as gates can be located along the navigation reaches, as well as secondary inputs. Therefore, they cannot be considered as a single reach with only two controlled points, the upstream and the downstream ends. This particularity demands a decomposition of the reaches in several sub-reaches according to the hydraulic structures and secondary inputs that affect the water stream. The models that represent the influence of the discharges on the water levels for each sub-reach have to be computed. The next step is to interconnect these partial models to reproduce the behavior of the whole canal. In this work, this modeling step is based on IDZ models. However, this modeling procedure might cause the flow profiles for each of these partial models to be not consistent with the flow profiles of the adjacent sub-reaches. This means that the interconnected model will most probably not reproduce adequately the real dynamics of the whole reach. This work aims to develop a modeling approach in which the prior knowledge of the whole system dynamics are taken into account when each of these sub-reaches is modeled.

The content of this paper is structured as follows: Section 2 is dedicated to the description of the IDZ model. Section 3 addresses the modeling step of two sub-reach systems introducing some considerations as well as the interconnection method. In Section 4, the proposed approach is used by considering a real navigation reach located in the north of France, the Cuinchy-Fontinettes reach. The comparison of the interconnection approaches with and without prior knowledge of the whole system with a reference model is performed. This reference model is provided by an hydraulic simulation software that solves numerically the Saint-Venant equations. Finally, conclusions about the performed work are drawn in Section 5.

2 SELECTING A MODEL TO DESCRIBE A REACH

As already mentioned, the Saint-Venant differential equations accurately describe the real dynamics of the system. However, since no analytical solution is known for these equations, as well as being extremely sensitive to errors in the geometry and other unmodeled dynamics, simplified models are needed. Among all the existing possibilities, the IDZ model (Litrico and Fromion, 2004) is used in this paper. It results from the linearization of the Saint-Venant's differential equations around an operating point q_{op}, and constitutes a simple yet efficient option to accurately describe a canal in high and low regimes.

The IDZ model, as its name implies, consists of an integrator, a delay and a zero: the two first terms capture the low frequencies tank-like behavior, whereas the zero accounts for the high frequencies. In Laplace form, its structure is as follows:

$$p_{ij}(s) = \frac{\alpha_{ij}s+1}{\mathcal{A}_{ij}s} e^{-\tau_{ij}s}, \tag{1}$$

where α_{ij} represents the inverse of the zero, $\mathcal{A}_{ij}$ the integrator gain and τ_{ij} the propagation time delay. The exact values of these parameters cannot be computed, but an accurate approximation can be used instead (Litrico and Fromion, 2004). Since the used parameters are an approximation of the theoretical ones, the notation $\hat{p}_{ij}(s)$ replaces $p_{ij}(s)$ hereinafter.

The integrator gain illustrates how the volume changes according to the variation of the water level. This parameter is also known as the equivalent backwater area due to its dimensions. The time delay represents the minimum required time for a perturbation to travel from its origin to the measurement points. The zero approximates through a constant gain the oscillatory phenomena that occurs in high frequencies.

The model representing the influence of the discharges on the water levels at the boundaries is given by:

$$\begin{bmatrix} y(0,s) \\ y(L,s) \end{bmatrix} = \underbrace{\begin{bmatrix} \hat{p}_{11}(s) & \hat{p}_{12}(s) \\ \hat{p}_{21}(s) & \hat{p}_{22}(s) \end{bmatrix}}_{\boldsymbol{P}(s)} \begin{bmatrix} q(0,s) \\ q(L,s) \end{bmatrix}, \tag{2}$$

where 0 and L are the abscissas for the initial and final ends of the reach; $\hat{p}_{ij}(s)$, the IDZ model that links the i^{th} water level and the j^{th} discharge and follows the structure given in (1); $y(0,s)$ and $y(L,s)$, the upstream and downstream water levels, respectively; $q(0,s)$ and $q(L,s)$, the upstream and downstream discharges, respectively.

In order to compute α_{ij}, $\mathcal{A}_{ij}$ and τ_{ij} (with $i,j = 1,2$), it is necessary to know where the transition between the upstream uniform and downstream backwater flows occurs. The value of this abscissa is named x_1 and can be obtained as follows:

$$x_1 = \begin{cases} max\left\{L - \frac{y_L - y_n}{s_L}, 0\right\} & if s_L \neq 0 \\ L & if s_L = 0 \end{cases}, \tag{3}$$

with y_L $[m]$ the downstream boundary condition, y_n $[m]$ the normal depth and s_L (dimensionless) the deviation from bed slope of the line tangent to the water curve at the downstream end of the pool. The reader is referred to (Litrico and Fromion, 2004) for further details about the computation of these magnitudes.

According to (3), x_1 can either be 0, L or take an intermediate value between 0 and L. The reach is completely under backwater flow if $x_1 = 0$, completely under uniform flow if $x_1 = L$ or present both kinds of flow if $0 < x_1 < L$. In particular, the interval (0,x_1) is under uniform flow whereas the interval (x_1, L) is under backwater flow. This is an important fact for the computation of the parameters α_{ij}, $\mathcal{A}_{ij}$ and τ_{ij}, as they have to be computed for each kind of flow that is present in the reach. The same formulas are applied for the uniform and backwater parts but are evaluated according to the length of each of these parts. The partial uniform and backwater parameters are merged into the so-called equivalent parameters, which represent the whole pool. In the event that $x_1 = 0$ or $x_1 = L$, they will only have to be computed once, for the whole length of the reach.

Finally, the following consideration serves to introduce the problem that is studied in this work, which is no other than the presence of secondary inputs in a canal; in particular, the relative position of x_1 and the abscissa in which the inflow takes place (x_{inflow} hereinafter). The two possibilities are depicted in Fig. 1.

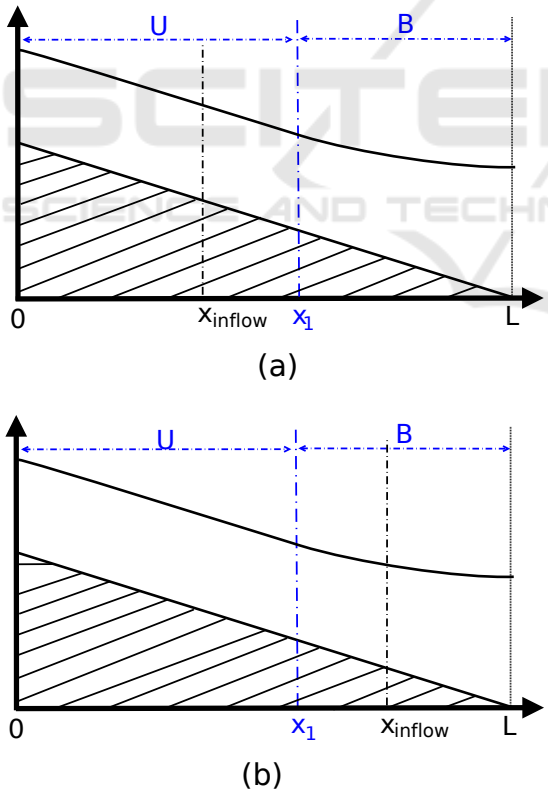

Figure 1: (a) Water profile for $x_1 > x_{inflow}$. (b) Water profile for $x_1 < x_{inflow}$.

The same water profile is obtained for both cases as the upstream and downstream boundary conditions are the same. The difference, however, appears when the whole reach is regarded as the interconnection of two sub-reaches due to the presence of the inflow. Fig. 1(a) is composed of a first sub-reach which is only under uniform flow and a second sub-reach under uniform flow in the interval (x_{inflow}, x_1) and backwater flow in the interval (x_1, L). On the other hand, Fig. 1(b) shows that the first sub-reach is under uniform flow in the interval (0, x_1) and under backwater flow in the interval (x_1, x_{inflow}) whereas the second sub-reach is only under backwater flow.

The objective, therefore, is to compute the IDZ model as an interconnection of two sub-reaches divided by a secondary inflow within the ends of the reach.

3 MODELING A TWO SUB-REACH SYSTEM

In this section, the general formulation of interconnected sub-reaches (Litrico and Fromion, 2004) is given. It is then extended by considering different criteria regarding the use of the previous knowledge of the global dynamics. Two different interconnected models are proposed and discussed.

3.1 Formulation of the Interconnected IDZ Model

One possible approach to model the systems that were presented in Fig. 1 is to consider two different sub-reaches. This division of a reach into sub-reaches is always done when there is an hydraulic structure that physically divides the reach, but also under other circumstances, *i.e.* the presence of a secondary input or a change in the cross section of the the water stream. Moreover, since there is no such hydraulic structure, this situation is hereinafter referred to as *simple interconnection*. Fig. 2 (where big-sized markers at sections 0 and L denote the presence of an hydraulic structure) illustrates this situation. For the sake of convenience, 0, x_{inflow} and L denote the initial, intermediate (where the inflow takes place) and final abscissas of the reach, respectively.

From relation (2), and according to Fig. 2, the following set of equations can be considered. SR_1 and SR_2 denote sub-reaches 1 and 2, respectively.

$$SR_1 : \begin{bmatrix} y(0,s) \\ y(x_{inflow},s) \end{bmatrix} = \begin{bmatrix} \hat{p}_{11}^{(1)}(s) & \hat{p}_{12}^{(1)}(s) \\ \hat{p}_{21}^{(1)}(s) & \hat{p}_{22}^{(1)}(s) \end{bmatrix} \begin{bmatrix} q(0,s) \\ q(x_{inflow},s) \end{bmatrix} \quad (4)$$

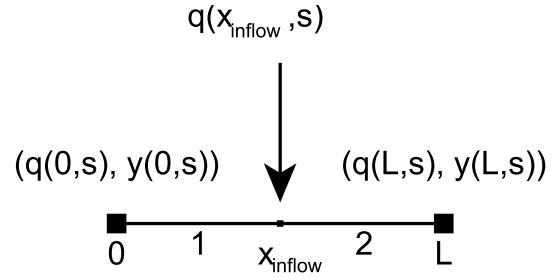

Figure 2: Water inflow flowing into a canal, leading to a simple interconnection structure.

$$SR_2 : \begin{bmatrix} y(x_{inflow},s) \\ y(L,s) \end{bmatrix} = \begin{bmatrix} \hat{p}_{11}^{(2)}(s) & \hat{p}_{12}^{(2)}(s) \\ \hat{p}_{21}^{(2)}(s) & \hat{p}_{22}^{(2)}(s) \end{bmatrix} \begin{bmatrix} q(x_{inflow},s) \\ q(L,s) \end{bmatrix} \quad (5)$$

This paper studies the particular case in which $q(x_{inflow}) = 0$, which can occur, for instance, when a lateral hydraulic device such as a controlled valve is closed and does not let the water flow into the main stream. The more general case $q(x_{inflow}) \neq 0$, *i.e.* when the controlled valve is open, will be addressed in the future.

For the case $q(x_{inflow}) = 0$, the final model that represents the interconnection is obtained by imposing the following conditions at the interconnection node (Litrico and Fromion, 2004):

$$y^{(1)}(x_{inflow},s) = y^{(2)}(x_{inflow},s) \quad (6a)$$

$$q^{(1)}(x_{inflow},s) = q^{(2)}(x_{inflow},s) \quad (6b)$$

These two equations express the continuity conditions that hold true at the interconnection abscissa x_{inflow}. In particular, Eq. (6a) ensures that no sudden change in the water depth occurs, whereas Eq. (6b) guarantees the flow consistency in the abscissa x_{inflow} and is a direct consequence of $q(x_{inflow}) = 0$.

Therefore, the final model (2) that represents the two interconnected sub-reaches is given by:

$$\begin{bmatrix} y(0,s) \\ y(L,s) \end{bmatrix} = \begin{bmatrix} \hat{p}_{11}^{(G)}(s) & \hat{p}_{12}^{(G)}(s) \\ \hat{p}_{21}^{(G)}(s) & \hat{p}_{22}^{(G)}(s) \end{bmatrix} \begin{bmatrix} q(0,s) \\ q(L,s) \end{bmatrix} \quad (7)$$

where $\hat{p}_{ij}^{(G)}$ represent the interconnecting transfer functions. Their expressions are:

$$\hat{p}_{11}^{(G)} = \hat{p}_{11}^{(1)} + \frac{\hat{p}_{12}^{(1)}\hat{p}_{21}^{(1)}}{\hat{p}_{11}^{(2)} - \hat{p}_{22}^{(1)}} \quad (8a)$$

$$\hat{p}_{12}^{(G)} = -\frac{\hat{p}_{12}^{(1)}\hat{p}_{12}^{(2)}}{\hat{p}_{11}^{(2)} - \hat{p}_{22}^{(1)}} \quad (8b)$$

$$\hat{p}_{21}^{(G)} = \frac{\hat{p}_{21}^{(1)}\hat{p}_{21}^{(2)}}{\hat{p}_{11}^{(2)} - \hat{p}_{22}^{(1)}} \quad (8c)$$

$$\hat{p}_{22}^{(G)} = \hat{p}_{22}^{(2)} - \frac{\hat{p}_{12}^{(2)}\hat{p}_{21}^{(2)}}{\hat{p}_{11}^{(2)} - \hat{p}_{22}^{(1)}} \quad (8d)$$

Note: the Laplace variable s has been omitted for readability in all $\hat{p}_{ij}^{(k)}$ terms.

In order to obtain the global model for the two sub-reach system, it seems it might be enough to compute a separate model for each sub-reach and then use (8a)–(8d) to obtain the interconnected model. The model obtained by means of this procedure is hereinafter referred to as a two sub-reach system with independent flow profiles.

However, as the two sub-reaches are not divided by any hydraulic structure, it does not seem correct to treat them independently. Instead, since $q(x_{inflow}) = 0$ in this paper, it is possible to obtain the value of x_1 for the whole canal and use this information when modeling each of the two sub-reaches. The model that is obtained by using this information about the global dynamics is hereinafter referred to as a two sub-reach system with consistent flow profile.

3.2 Two Sub-reach Systems with Independent Flow Profiles

The first and simplest option is to compute the model for each sub-reach separately according to the procedure described in Section 2 and then interconnect them. However, since there is no hydraulic structure dividing the two sub-reaches, a consistent flow profile is not obtained, which does not seem logical. This is caused by the need to compute x_1 for each sub-reach, which will probably result in obtaining a different flow profile with a completely different dynamic response. This idea is depicted in Fig. 3(a) and 4(a): a value of x_1 is computed for each sub-reach (blue dash-dot lines), which results in a completely different profile than the real one, shown in Fig. 1.

3.3 Two Sub-reach Systems with Consistent Flow Profiles

In this approach, the value of x_1 computed for the reach is used to build the interconnected two sub-reach system model afterward. The first sub-reach is forced to change from uniform to backwater flow in x_1 when $x_1 < x_{inflow}$, whereas in the situation $x_1 > x_{inflow}$ the second sub-reach is forced from uniform to backwater flow in x_1. This behavior is shown in Fig. 3(b) and 4(b), which results in the same curves as those depicted in Fig. 1.

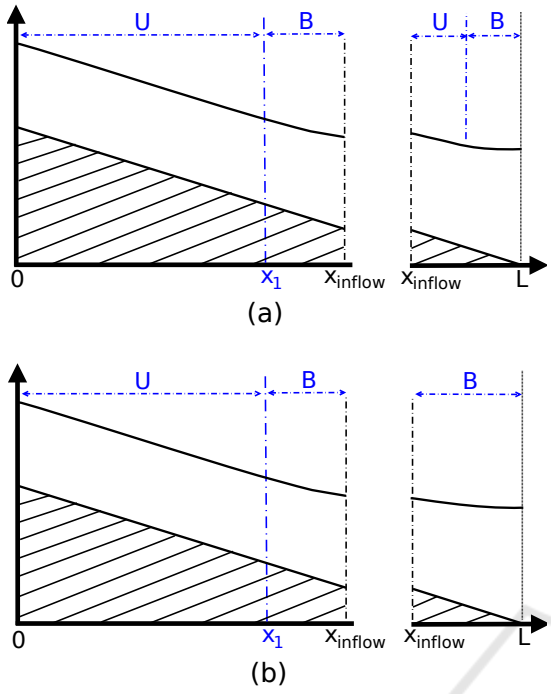

Figure 3: Flow profiles for a two-reach system when $x_1 < x_{inflow}$. (a) Independent flow profile. (b) Consistent flow profile.

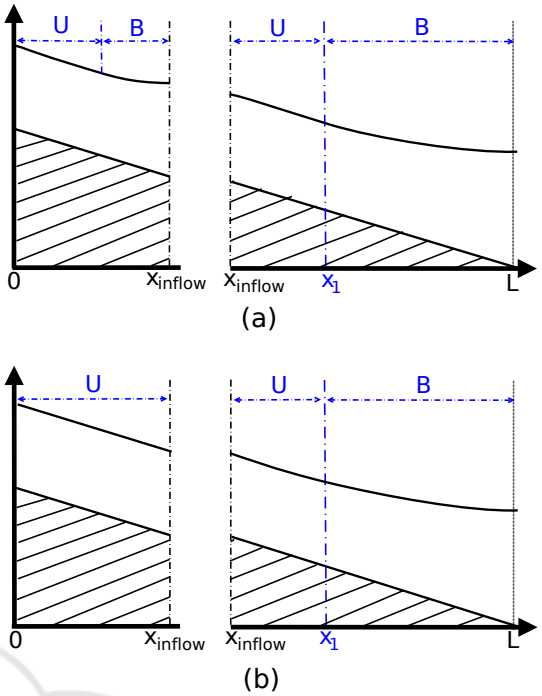

Figure 4: Flow profiles for a two-reach system when $x_1 > x_{inflow}$. (a) Independent flow profile. (b) Consistent flow profile.

4 APPLICATION

The aim is to verify which of the two approaches presented in Section 3 leads to a better model, even if one has the intuition that taking into account the previous knowledge of the system to ensure the flow continuity should yield better results than treating them as two sub-reaches with independent flow profiles. In order to compare them, both models are computed for a real system and then compared with the results provided by SIC^2 [2] (Malaterre et al., 2014), an hydraulic simulation software. Since it solves numerically the Saint-Venant equations without simplifications, the obtained results with this software will be used as the basis to compare the accuracy of both approaches.

The chosen two sub-reach system is the Cuinchy-Fontinettes reach (CFr), which belongs to the inland navigation network in the north of France and is illustrated in Fig. 5. This reach is bounded both upstream and downstream by the locks of Cuinchy and Fontinettes, respectively. The gate Port de Garde, which is located within both ends and placed outside of the CFr, can be used to regulate the amount of water that is sent to Aire. According to the current management strategy, this gate is generally closed, which is the reason why this value is considered to be equal to 0 in this work. The discharges in the locks of Cuinchy and Fontinettes are considered as the inputs of the IDZ model given by (2). On the other hand, they are modeled as discharge boundary conditions in SIC^2.

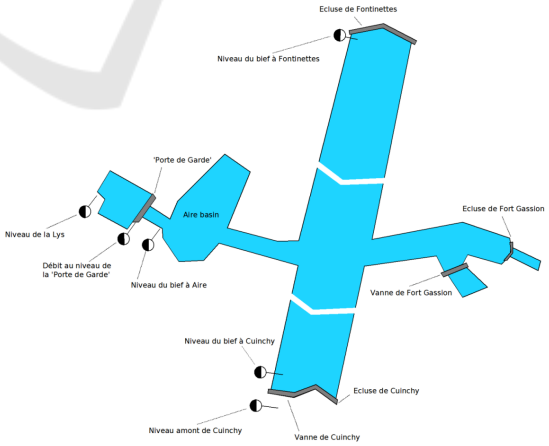

Figure 5: Schematic view of the CFr.

Table 1 sums up the physical and geometrical data used to model the CFr: n_r $[s/m^{1/3}]$ is the Manning's roughness coefficient, m (dimensionless) is the side slope of the cross section ($m = 0$ for rectangular shape), B_w $[m]$ is the bottom width of the reach, q_{op}

[2]http://sic.g-eau.net/

$[m^3/s]$ is the considered flow for the linearization of the Saint-Venant equations, L $[m]$ is the length and y_x $[m]$ is the downstream water depth. Besides, the bottom slope s_b is equal to 10^{-4} for both reaches. On the other side, C, A and F stand for Cuinchy, Aire and Fontinettes, respectively.

Table 1: Physical data for CFr.

	n_r	m	B_w	q_{op}	L	y_x
C-A	0.035	0	52	0.6	28700	2.44
A-F	0.035	0	52	0.6	13600	3.8
C-F	0.035	0	52	0.6	42300	3.8

Two real scenarios are considered: the first one presents the operation of the Cuinchy lock; the second one, the operation of the Fontinettes lock. Table 2 contains the details of these lock operations. A positive sign for the dispatched water volume means that the water volume is flowing into the system, whereas a negative sign means that it is leaving the system.

Table 2: Considered scenarios.

Scenario	Volume $[m^3]$	Duration $[min]$
1	3000	15
2	-23000	20

The following fit coefficients are computed (between the reference and each of the proposed models) for a quantitative comparison of the accuracy of the results:

- *Pearson product-moment correlation coefficient*, which measures the linear dependance between two variables. It is defined in the following way:

$$r = \frac{\sum_{t=1}^{T} \left(Y_o(t) - \overline{Y_o}\right)\left(Y_m(t) - \overline{Y_m}\right)}{\sqrt{\sum_{t=1}^{T} \left(Y_o(t) - \overline{Y_o}\right)^2}\sqrt{\sum_{t=1}^{T} \left(Y_m(t) - \overline{Y_m}\right)^2}} \quad (9)$$

  with T the horizon for which the data have been acquired, $Y_o(t)$ the observed water depth at time t, $Y_m(t)$ the predicted water depth at time t and $\overline{Y_o}$ and $\overline{Y_m}$ the mean value of observed and modeled water depths, respectively.

  This coefficient is bounded between +1 (total positive linear correlation) and -1 (total negative linear correlation), and 0 means that there is no linear correlation.

- *Nash-Sutcliffe model efficiency coefficient*, which is used to assess the predictive power of hydrological models as follows (Nash and Sutcliffe, 1970):

$$E = 1 - \frac{\sum_{t=1}^{T} \left(Y_o(t) - Y_m(t)\right)^2}{\sum_{t=1}^{T} \left(Y_o(t) - \overline{Y_o}\right)^2} \quad (10)$$

  E can range from 1 to $-\infty$, where 1 indicates a perfect match of modeled and observed values, 0 corresponds to the case in which the model predictions are as accurate as the mean of observed data and $E < 0$ means that the model predictions are less accurate than the mean of observed data.

- *Maximum difference between the modeled and observed data* as a measure of the magnitude of the maximum error. It is computed as:

$$\Delta = \max_{1 \le t \le T} |Y_o(t) - Y_m(t)| \quad (11)$$

The results for both scenarios are presented below. For each of them, the previous fit coefficients between the reference (SIC^2) and the three different modeling approaches (model of the reach, two sub-reaches with independent and consistent flow profiles) are summarized in Tables 3 and 4. In addition, the simulation results for Y_C and Y_F are presented for the four models. Each figure is zoomed in the area of interest; however, the same simulation time has been used for both scenarios.

Remark: the computation of the IDZ model for the reach results in $x_1 = 5760\ m$, which indicates that the present case study falls under the situation described by Fig. 3 as $x_{inflow} = 28700\ m$. This means that the C-A reach is under both uniform and backwater flow (with flow transition at $x = x_1$) and that A-F is under backwater flow only. On the other hand, the obtained profile for the two-reach model with independent flow profile is only backwater for both of them: when the IDZ model is computed for each sub-reach, a value of $x_1 = 0$ is obtained for both sub-reaches, which means that they are both under backwater.

4.1 Scenario 1

Figures 6 and 7 and Table 3 summarize the results obtained for the Cuinchy lock operation.

Table 3: Fit coefficients for an upstream lock operation.

		Reach	Indep. flow	Cont. flow
C	E_C	0.2831	-0.0193	0.2831
	r_C	0.7311	0.4328	0.7312
	$\Delta_C\ [m]$	0.1225	0.1703	0.1272
F	E_F	-1.2637	-5.3193	-1.0506
	r_F	0.5110	0.0641	0.5613
	$\Delta_F\ [m]$	0.0016	0.0128	0.0015

None of the three models is capable of representing the observed peak in Y_C with satisfying accuracy,

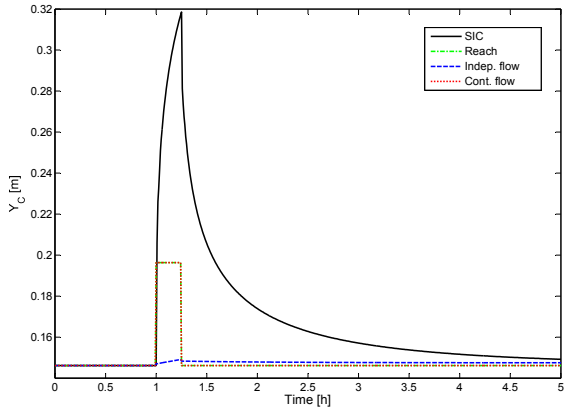

Figure 6: Upstream water levels for an upstream lock operation.

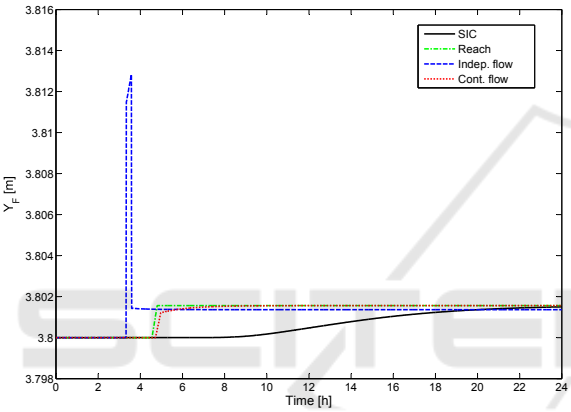

Figure 7: Downstream water levels for an upstream lock operation.

even if the equilibrium value is well fitted. Nevertheless, the consistent flow profile model, which is overlapped with the reach model, offers a better peak response than the two sub-reach model with independent flow profile.

Moreover, the two sub-reach model with independent flow profile clearly predicts a much worse response for Y_F than the other two models, represented by the nonexistent predicted peak according to the reference. The appearance of this peak is physically justified by the fact that the computation of the flow profile for the two sub-reach system with independent flow yields backwater flow only. The systems that exhibit this kind of flow profile are more sensitive to resonance phenomena. An example of this behavior was obtained in a work with flat systems (Segovia et al., 2017).

It is also worth noting that both the reach model and the consistent flow profile model predict a much faster response than it is actually observed, which causes the Nash-Sutcliffe indicators to be negative for Y_F. Nevertheless, when the consistent flow model is considered, the maximum difference is lower and the dynamics are better reproduced, as shown by the computed correlation coefficients.

4.2 Scenario 2

In this case, Figures 8 and 9 and Table 4 summarize the results for the Fontinettes lock operation.

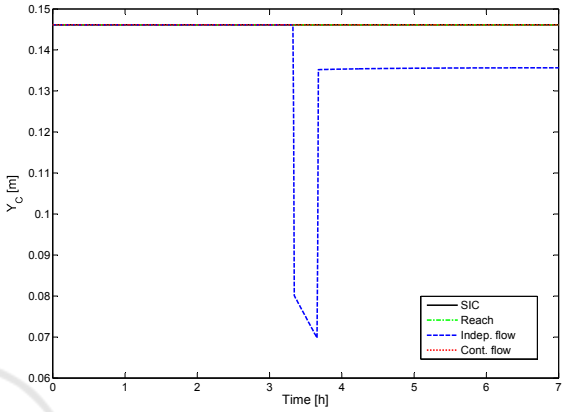

Figure 8: Upstream water levels for a downstream lock operation.

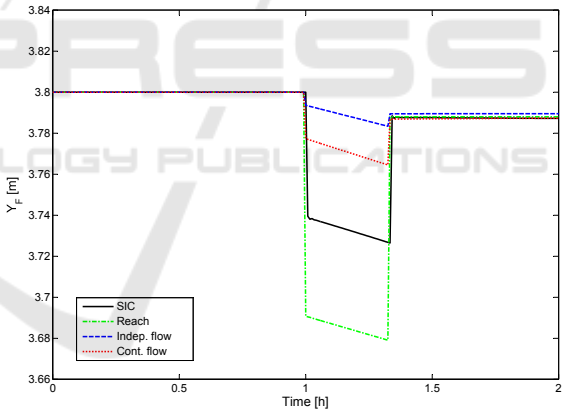

Figure 9: Downstream water levels for a downstream lock operation.

For the upstream level Y_C, the flat signal corresponds to the overlapping of the observed water depths and the predicted responses with the reach model and the consistent flow model. This fact is shown by the maximum difference indicator in Table 4, which prevents the computation of the Nash-Sutcliffe indicators for these two models. The two sub-reach model with independent flow profile predicts a very different response from the observed data. Indeed, a peak is predicted in the response of the two sub-reach system with independent flow profile, whose justification is the same as given for Y_F in Section 4.1. The Nash-Sutcliffe indicator takes an ex-

Table 4: Fit coefficients for a downstream lock operation.

		Reach	Indep. flow	Cont. flow
C	E_C	—	-3.38 $\cdot 10^9$	—
	r_C	0.3894	0.2388	0.3785
	Δ_C $[m]$	0	0.0764	0
F	E_F	0.2394	0.0444	0.5671
	r_F	0.9549	0.4370	0.8607
	Δ_F $[m]$	0.0471	0.0630	0.0383

tremely large, negative value, showing the deviation between this model and the observed values.

With regard to Y_F, the predicted dynamics for the three models are similar, albeit the reach model and the consistent flow profile models offer a better prediction than the other model.

A conclusion for both scenarios is that an operation performed at one end of the system does not have a major impact at the other end, which is due to the large dimension of the system. Another factor that might play a role in this behavior is the fact that a bed slope equal to 10^{-4} is considered, which results in different values for the upstream and downstream bottom elevation. For the second scenario, a large volume of water is dispatched outside the system, and the observed data show that the water level remains (almost) constant upstream. The final water level variation is due to the mass balance along the system.

Another conclusion that can be drawn for both scenarios is that the two sub-reach model with independent flow profile predicts significant peaks in Y_F for the upstream action and in Y_C for the downstream action results from considering two backwater flow dynamics. If a system has to be modeled as the interconnection of two sub-reaches, the best choice seems to consider the consistent flow profile model.

5 CONCLUSIONS AND FUTURE WORK

This work presented the study of a two sub-reach system based on IDZ models. Some considerations that need to be taken into account in order to ensure the flow consistency of the system were addressed, and those steps were illustrated by means of a case study based on a real system in the north of France. According to the obtained results, it is possible to state, as one could previously anticipate, that the accuracy with respect to the reference is greater if the previous knowledge of the system (namely x_1) is considered to ensure the continuity of the flow.

In the light of the outcome, although the IDZ model yields acceptable results, other aspects may need to be considered to possibly come up with some rules about its applicability. Further work includes addressing the general case $q(x_{inflow}) \neq 0$. In this case, the structure of the global model (2) will be different, but the modeling approach will be similar. In addition, canals characterized by a different topography such as tributaries and distributaries will be considered. The obtained models are expected to be used in fault detection and isolation (FDI) and fault-tolerant control (FTC).

REFERENCES

Bolea, Y. and Puig, V. (2016). Gain-scheduling multivariable LPV control of an irrigation canal system. *ISA Transactions*, 63:274–280.

Bolea, Y., Puig, V., and Blesa, J. (2014). Linear parameter varying modeling and identification for real-time control of open-flow irrigation canals. *Environmental modelling & software*, 53:87–97.

Chow, V. T. (1959). Open-channel hydraulics. *McGraw-Hill. New York.*

Duviella, E., Bako, L., and Charbonnaud, P. (2007). Gaussian and boolean weighted models to represent variable dynamics of open channel systems. *Conference on Decision and Control, New Orleans, USA, December 12-14*.

Duviella, E., Bako, L., Sayed-Mouchaweh, M., Blesa, J., Bolea, Y., Puig, V., and Chuquet, K. (2013). Inland navigation channel model: Application to the Cuinchy-Fontinettes reach. In *Networking, Sensing and Control (ICNSC), 2013 10th IEEE International Conference on*, pages 164–169. IEEE.

Duviella, E., Puig, V., Charbonnaud, P., Escobet, T., Carrillo, F., and Quevedo, J. (2010). Supervised gain-scheduling multimodel versus linear parameter varying internal model control of open-channel systems for large operating conditions. *Journal of Irrigation and Drainage Engineering*, 136(8):543–552.

Horváth, K., Duviella, E., Blesa, J., Rajaoarisoa, L., Bolea, Y., Puig, V., and Chuquet, K. (2014a). Gray-box model of inland navigation channel: application to the Cuinchy-Fontinettes reach. *Journal of Intelligent Systems*, 23(2):183–199.

Horváth, K., Duviella, E., Petreczky, M., Rajaoarisoa, L., and Chuquet, K. (2014b). Model predictive control of water levels in a navigation canal affected by resonance waves. *HIC 2014, New York, USA, 17-21 August*.

Litrico, X. and Fromion, V. (2004). Simplified modeling of irrigation canals for controller design. *Journal of Irrigation and Drainage Engineering*, pages 373–383.

Litrico, X. and Georges, D. (1999). Robust continuous-time and discrete-time flow control of a dam–river system. (I) Modelling. *Applied mathematical modelling*, 23(11):809–827.

Malaterre, P.-O., Baume, J.-P., and Dorchies, D. (2014). Simulation and integration of control for canals software (sic 2), for the design and verification of manual or automatic controllers for irrigation canals. In *USCID Conference on Planning, Operation and Automation of Irrigation Delivery Systems*, pages 377–382.

Nash, J. E. and Sutcliffe, J. V. (1970). River flow forecasting through conceptual models part I: a discussion of principles. *Journal of hydrology*, 10(3):282–290.

Schuurmans, J., Clemmens, A., Dijkstra, S., Hof, A., and Brouwer, R. (1999). Modeling of irrigation and drainage canals for controller design. *Journal of Irrigation and Drainage Engineering, December*, 125(6).

Segovia, P., Blesa, J., Horváth, K., Rajaoarisoa, L., Nejjari, F., Puig, V., and Duviella, E. (2017). Fault detection and isolation in flat navigation canals. 4^{th} *International Conference on Control, Decision and Information Technologies, April 5–7, Barcelona, Spain*.

van Overloop, P., Horváth, K., and Aydin, B. E. (2014). Model predictive control based on an integrator resonance model applied to an open water channel. *Control Engineering Practice*, 27:54–60.

van Overloop, P., Miltenburg, I., Bombois, X., Clemmens, A., Strand, R., van de Giesen, N., and Hut, R. (2010). Identification of resonance waves in open water channels. *Control Engineering Practice, Volume 18, Issue 8, August*, pages 863–872.